The inertial regimes in Rayleigh-Bénard convection. Les régimes inertiels de la convection de Rayleigh-Bénard

Bernard Castaing, Francesca Chillà, Julien Salort, Yann Fraigneau, Anne Sergent

ACADÉMIE DES SCIENCES
INSTITUT DE FRANCE

Comptes Rendus. Physique
Draft

Research article / *Article de recherche*

The inertial regimes in Rayleigh-Bénard convection.

Les régimes inertiels de la convection de Rayleigh-Bénard

Bernard Castaing [a], Francesca Chillà [*,b], Julien Salort [b], Yann Fraigneau [c] and Anne Sergent [c]

[a] Laboratoire des écoulements géophysiques et industriels, Domaine Universitaire, CS 40700, 38058 Grenoble Cedex 9, France

[b] ENSL, CNRS, Laboratoire de physique, F-69342 Lyon, France.

[c] Université Paris-Saclay, CNRS, Laboratoire Interdisciplinaire des Sciences du Numérique, F91405 Orsay, France

E-mail: francesca.chilla@ens-lyon.fr

Abstract. Most theoretical studies of Rayleigh- Bénard Convection assume that the velocity boundary layer develops on the whole width or height H of the convection cell, or that the development length h scale with H. We argue that it is probably not the case, and examine the consequences of an intermediate asymptotics hypothesis in the sense of Barenblatt [1], the development length h scaling with the Nusselt number: $h \propto HNu^{-\alpha}$. This hypothesis is checked through existing experimental data, which show that α can take several different values. The analysis of Grossmann and Lohse [2] is reexamined with this new point of view, stressing on pure scaling regimes.

Résumé. La plupart des études théoriques sur la convection de Rayleigh-Bénard supposent que la couche limite de vitesse se développe sur toute la largeur ou la hauteur H de la cellule de convection, ou que la longueur de développement h est proportionnel à H. Nous soutenons qu'il est probablement incorrect de faire cette supposition, et nous examinons les conséquences d'une hypothèse d'asymptotique intermédiaire au sens de Barenblatt [1], où la longueur de développement h dépend du nombre de Nusselt: $h \propto HNu^{-\alpha}$. Cette hypothèse est vérifiée à partir de données expérimentales existantes, qui montrent que α peut prendre plusieurs valeurs différentes. L'analyse de Grossmann et Lohse [2] est réexaminée sous cette nouvelle perspective, en mettant l'accent sur les régimes d'échelle pure.

Keywords. Turbulence, Convection.

This article is a draft (not yet accepted)

* Corresponding author

1. Introduction.

Convection is ubiquitous. Among other important problems, it governs the behavior of stars, the climate of planets, or the behavior of the molten core in a damaged nuclear plant. However, the bridge between these large scale events and their laboratory counter part, the Rayleigh-Bénard convection cell is not yet firmly set.

The Rayleigh-Bénard convection cell consists in a Newtonian, nearly incompressible, isotropic fluid, of kinematic viscosity ν, of heat diffusivity κ, of thermal expansion β, put into motion by a vertical heat flux $\dot{Q}$. The problem is generally treated within the Boussinesq approximation, whose equations write:

$$\partial_t v_i + v_j \partial_j v_i = -\frac{1}{\rho}\partial_i p + g_i \beta\theta + \nu \partial_j \partial_j v_i, \tag{1}$$

$$\partial_j v_j = 0, \tag{2}$$

$$\partial_t \theta + v_j \partial_j \theta = \kappa \partial_j \partial_j \theta, \tag{3}$$

where g_i and v_i are the i components of the gravitational acceleration and the velocity, and θ is the temperature.

The non dimensional control parameters are the Rayleigh number:

$$Ra = \frac{g\beta\Delta H^3}{\nu\kappa} \tag{4}$$

where g is the gravitational acceleration, Δ the temperature difference between the horizontal plates, the hot one (generally below) and the cold one, H the vertical distance between these plates. Of importance are also the Prandtl number:

$$Pr = \frac{\nu}{\kappa} \tag{5}$$

and the parameters specifying the shape of the cell, as the aspect ratio:

$$\Gamma = \frac{L}{H} \tag{6}$$

where L is the typical horizontal dimension of the plates.

The non dimensional parameters measuring the answer of the cell are the Nusselt number:

$$Nu = \frac{\dot{Q}H}{C_p \kappa \Delta} \tag{7}$$

where C_p is the isobaric heat capacity of the fluid per unit volume. The Reynolds number:

$$Re = \frac{UH}{\nu} \tag{8}$$

where U is a typical velocity of the fluid, and the relative temperature fluctuations:

$$Ft = \frac{\Theta}{\Delta} \tag{9}$$

where Θ^2 is the variance of the temperature fluctuations, generally depend on the way and the point where the measures of U and Θ are made, but are nethertheless precious indications of the nature of the flow.

During the second half of the past century, many propositions have been made for the Ra dependence of Nu, most of them as a power law (for a review, see [2], [3], [4] and [5]):

$$Nu = Ra^{\mu} \tag{10}$$

with occasional logarithmic corrections. Absolute majoration have been derived [6], showing that, whatever the Prandtl number, in the limit of large Ra:

$$Nu < CRa^{1/2} \tag{11}$$

where C is a constant.

Within approximately the same period, a great number of experiments ([2], [3], [4]) have been performed, including numerical experiments, reaching up to $Ra = 10^{17}$, generally analyzed as power laws, equation 10, or a succession of power laws. It results in a wide variety of μ values proposed, both theoretically and experimentally.

In the past two decades, in a series of seminal papers, S. Grossmann and D. Lohse (GL) [7] have proposed to rely the predictions to two exact results concerning the viscous (ε) and thermal (ε_T) dissipations per unit volume:

$$\varepsilon = \nu < \partial_i v_j \partial_i v_j > = \frac{\kappa^3}{H^4} Ra(Nu-1)Pr, \tag{12}$$

$$\varepsilon_T = \kappa < \partial_i T \partial_i T > = \frac{\kappa \Delta^2}{H^2} Nu, \tag{13}$$

Remarking that each dissipation can be dominated either by the boundary layer or by the bulk, they proposed to classify the flows into four categories:

(I)	Both dissipations are dominated by the boundary layer
(II)	Thermal dissipation dominated by the boundary layer, viscous by the bulk
(III)	Viscous dissipation dominated by the boundary layer, thermal by the bulk
(IV)	Both dissipations are dominated by the bulk

Moreover, each category has the subscript "u" for the large Pr, and "l" for the small ones, and has a prime "$\prime$" if the boundary layer is turbulent. Evaluating the bulk and boundary layer dissipations, both viscous and thermal, and using the exact relations 12 and 13, GL could obtain the Nu and Re numbers in a wide range of intermediate values of Ra and Pr. *Ad hoc* cross-over functions, and adjustable parameters were necessary, fitted to the existing experimental results. As a result, as remarked by GL, none of the pure regimes described in the table 1 appears alone, the combination of two of them being undistinguishable from a pure power law as equation 10.

In this paper, we shall follow the same way, relying to the exact results 12 and 13, and evaluating the bulk and boundary layer dissipations. However, our approach will differ from the GL one on the following points:

- We shall take into account the various possible regimes, both in the bulk and in the boundary layer. We shall stress the influence of the so called mixing transition ([8], [9]) in the bulk, and we shall reinterpret the mixing buffer zone of Kadanoff *et al.* [10]
- We renounce to the dogma of single Nu or Re values for given Ra and Pr, even at a given aspect ratio, recognizing that minute details can select between a wealth of possible regimes.
- While recognizing the possibility of crossovers we shall stress on pure regimes, finding evidences of them in published experimental data.

The paper is organized as follows. In section 2, we shall check an hypothesis made in all models, that the product of the typical velocity and the typical temperature fluctuations well represents their cross-correlation, *i.e.* that their cross-correlation coefficient is constant. In section 3, we shall introduce the development length of the velocity boundary layer, and make the hypothesis of a simple scaling of this length with the Nusselt number. We shall examine how it influences the velocity and thermal boundary layers. In section 4, we shall check the above hypothesis. In section 5, we shall evaluate the viscous dissipation, in the boundary layer, distinguishing between Blasius or logarithmic ones, and in the bulk, distinguishing between soft and hard turbulence. This goes through a determination of the velocity boundary layer width, λ, which we use in section 6 for determining the thermal one δ. In section 7, we evaluate the thermal dissipation, particularly in the bulk, where we distinguish between soft and hard turbulence. In section 8, we use all our results for discussing some remarkable cases, before to conclude in section 9.

2. The cross-correlation between temperature and vertical velocity

We shall begin examining an assumption made by every model, the proportionality between the temperature and vertical velocity correlation $\langle v_z\theta\rangle$, and the product of the typical velocity U with the typical temperature fluctuation Θ. Noting that:

$$Nu = \frac{\langle v_z\theta\rangle\, H}{\kappa\Delta} \tag{14}$$

the coefficient of cross-correlation can be obtained as:

$$\chi = \frac{\langle v_z\theta\rangle}{U\Theta} = \frac{Nu}{RePr}\frac{\Delta}{\Theta} \tag{15}$$

Unfortunately, very few experimental or numerical work give simultaneous estimations of Nu, Re and temperature fluctuations for given Ra and Pr numbers. We had access to two of them: the PhD thesis of XZ Wu [11] and the work of Chavanne *et al.* [14]. For the later, we used unpublished complementary materials, namely long simultaneous records of two close by thermometers, whose cross-correlation allowed to determine the Reynolds number.

For both of these sets of data, we applied a correction to the Nusselt values, to take into account the finite heat conductivity of the walls. Indeed, Roche *et al.* [15], and independently Ahlers [16] realized that the influence of the walls is much larger than previously assumed. Roche *et al.* proposed a formula to derive the corrected Nusselt Nu from the raw one Nu_{raw}:

$$Nu = \frac{Nu_{raw}}{1+f} \tag{16}$$

where:

$$f = \frac{\mathscr{A}^2}{\Gamma Nu_{raw}}\left(\sqrt{1+\frac{2W\Gamma Nu_{raw}}{\mathscr{A}^2}}-1\right) \tag{17}$$

with $\mathscr{A}\simeq 0.8$, Γ is the aspect ratio (here $\Gamma = 0.5$), and the wall number W depends on the ratio of the heat conductivities of the wall and the fluid and the geometric dimensions of the wall. Here, we can use the value $W = 0.6$ corresponding to the small density He gas (low Nu). For the larger Nu, f is small: $f < 0.1$ when $Nu_{raw} > 100$ ($\ln(Nu_{raw}) > 4.6$). Then, a 50% error on W would result in 2% error on Nu.

We also used data from the work of Musilova *et al.* [17]. We obtained an estimation of Ft (9) for these data using a fit of their results, shown on their figure 6:

$$Ft_M = (0.433 + 0.0125\cdot log_{10}(Ra))Ra^{-1/7} \tag{18}$$

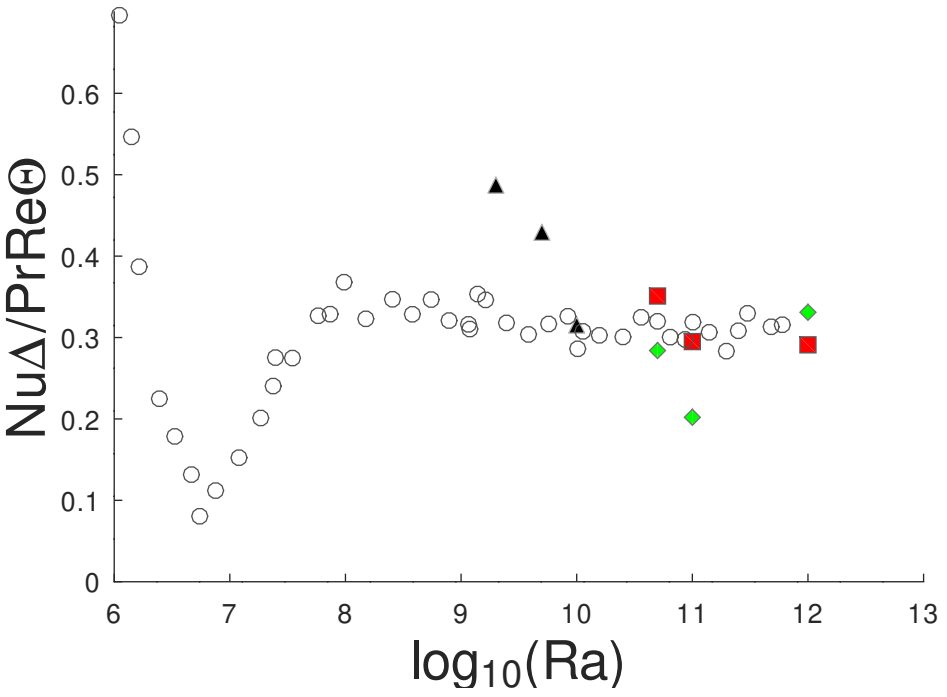

Figure 1. Open symbols: the "correlation coefficient" χ for the XZ Wu results [11]. Full symbols: the true correlation coefficient $\langle v_z\theta\rangle / \sqrt{\langle v_z^2\rangle \langle\theta^2\rangle}$ at various places for a numerical simulation of a rectangular Rayleigh-Bénard cell of dimensions $1, 0.25, 1$ [12, 13]. Black triangles: point $(0.25, 0.125, 0.5)$. Red squares: point $(0.35, 0.125, 0.5)$. Green diamonds: point $(0.5, 0.125, 0.5)$ (middle of the cell).

The data of Wu [11], figure 1, show large variations for $Ra < 10^8$, and an approximately constant value for larger Ra. We plot on the same figure the values of the local true correlation coefficient $\langle v_z\theta\rangle / \sqrt{\langle v_z^2\rangle \langle\theta^2\rangle}$ at various places for a numerical simulation of a rectangular Rayleigh-Bénard cell of dimensions $1, 0.25, 1$ [12,13]. The simulation again show two regimes, one variable, and one constant. The apparent agreement of the numerical values for the simulation and the Wu experiment is probably fortuitous. The succession of regimes in the simulation is more similar to the Musilova *et al.* [17] one (see figure 2). The remarkable point for the simulation is that the correlation in the center, where the fluctuations are very weak, is approximately the same as in much more active regions.

The data of Chavanne *et al.* [14], figure 2, show two plateaus, separated by a transition in the neighborhood of $Ra \simeq 3 \cdot 10^9$. The data of Musilova *et al.* [17] show large variations at low Ra, but are in close agreement with Chavanne *et al.* for $Ra > 10^{10}$.

We thus have different cases. In some ranges, the cross-correlation coefficient between velocity and temperature cannot be considered as constant. The basic assumption made in all the models thus fails. On the other hand, however, there are ranges where the cross-correlation coefficient is constant. The usual approaches can then be used.

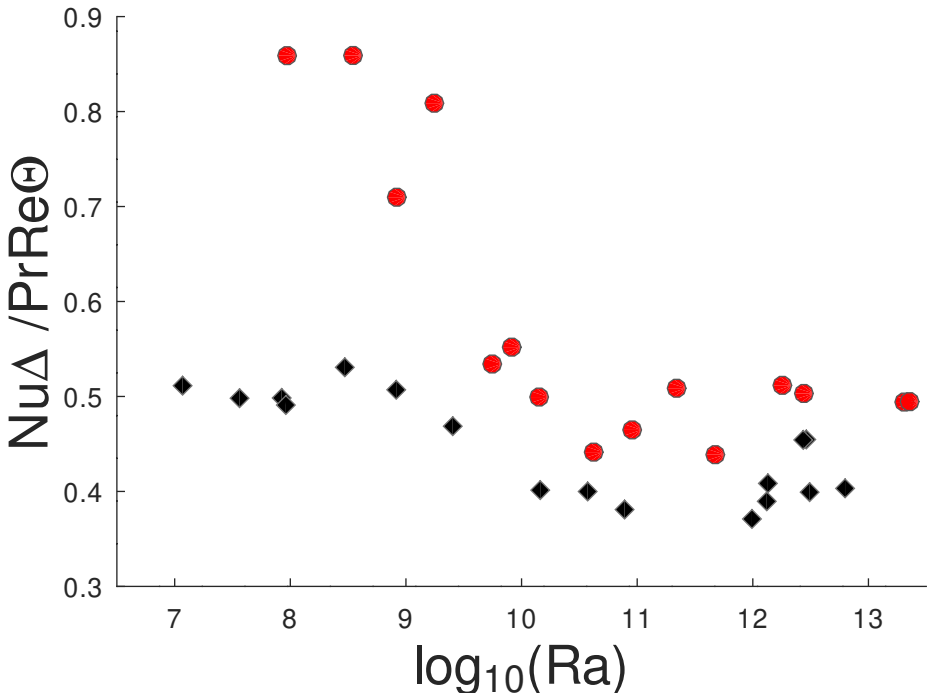

Figure 2. The correlation coefficient χ for the Chavanne *et al.* results [14], black diamonds, and the Musilova *et al.* ones [17], red circles

3. The thermal boundary layer. Influence of the development length

In this section, our analysis will be at variance with most of previous ones, which consider that the velocity boundary layers develop on the whole width or height of the cell. We shall explicitly introduce the development length h as a new parameter, and we shall assume that it is related to the Nusselt number as:

$$\frac{h}{H} = Nu^{-\alpha} \tag{19}$$

In all this paper, we shall renounce to precisely determine the constant factors, so our equality rather means proportionality. The above relation is inspired by the idea that the thermal boundary layer in some way governs the velocity one.

3.1. *Large Prandtl numbers*

To our knowledge, the only work which considers the possibility of a development length which differs from H is that of ESC Ching [18]. Ching solved the problem of the vertical (z) temperature profile within the velocity boundary layer, for large Prandtl number. Under some conditions, she found a self similar solution:

$$T - T_p = \Delta f(z/\delta(x)) \tag{20}$$

T_p being the temperature of the plate ($z = 0$), and x the velocity direction.

Rather than reproducing her argument, we propose to derive the typical value of δ from dimensional arguments. The x-component of the velocity has a linear profile:

$$u_x = \gamma z \tag{21}$$

The basic dimensions are $[x]$, $[z]$ (which we consider as independent) and the time $[t]$. δ depends on γ, the temperature diffusion coefficient κ, and the development length h. The dimensions are:

$$[u_x] = \frac{[x]}{[t]}, [\gamma] = \frac{[x]}{[t][z]}, [h] = [x], [\kappa] = \frac{[z]^2}{[t]}, [\delta] = [z] \tag{22}$$

Thus, within a numerical factor:

$$\delta = \left(\frac{\kappa h}{\gamma}\right)^{1/3} \tag{23}$$

The solution of Ching depends on two parameters, A and K, which are linked through $f(\infty) = 1/2$. For small K, A poorly depends on K, as $A = A_o(1 - BK^2)$ with B close to 1:

$$K = \delta' \simeq \frac{\delta}{h}, A = \frac{\delta(\gamma\delta^2)'}{2\kappa} \simeq \frac{\gamma\delta^3}{\kappa h} \tag{24}$$

$'$ means deriving versus x, which is equivalent to divide by h in our approach. We thus agree with the result of Ching, as far as K is not too large, which means h much larger than δ.

3.2. *Low Prandtl numbers*

Let us now remark that the above result, equation 23, is equivalent to postulate that a peculiar Peclet number is 1 at the limit of the thermal boundary layer. Within the velocity boundary layer, we can determine the vertical velocity component u_z through the mass conservation equation 2:

$$\partial_z u_z = -\partial_x u_x = \frac{\gamma}{h} z \tag{25}$$

Then $u_z(\delta) = \gamma\delta^2/h$ (we omit the factor 2), and:

$$Pe = \frac{u_z \delta}{\kappa} = \frac{\gamma\delta^3}{h\kappa} = 1 \tag{26}$$

As often postulated, the thermal boundary layer limit is the point where the Peclet number is 1. But we must remember that the velocity which enters this Peclet number is the vertical velocity.

We can apply this idea to the case of small Prandtl numbers, where the thermal boundary layer extends out of the velocity one. Then, equation 25 writes:

$$\partial_z u_z = -\partial_x u_x = \frac{U}{h} \tag{27}$$

Then $u_z(\delta) = U\delta/h$, and:

$$Pe = \frac{u_z \delta}{\kappa} = \frac{U\delta^2}{h\kappa} = 1 \tag{28}$$

At the velocity boundary layer limit, λ, we rather have $U\lambda^2/h\nu = 1$. The consequence is that

$$\lambda = \delta Pr^{1/2} \tag{29}$$

if $Pr < 1$, and

$$\lambda = \delta Pr^{1/3} \tag{30}$$

if $Pr > 1$.

3.3. *The transition between Large and Low Prandtl numbers*

The results of Ching allow to precisely determine the boundary between low and large Prandtl numbers. According to the Landau-Lifchitz texbook [34], within the Blasius model, the velocity gradient at the boundary is:

$$\gamma \simeq 0.332\sqrt{U^3/\nu x} = U/\lambda \tag{31}$$

Then, using equation 24:

$$2A\kappa = \delta\left(\gamma\delta^2\right)' = -\gamma'\delta^3 = \frac{\nu}{0.332^2}\left(\frac{\delta}{\lambda}\right)^3 \tag{32}$$

In the small K limit (where $h >> \delta$), Ching obtains $A \simeq 2.136$:

$$\left(\frac{\delta}{\lambda}\right)^3 = \frac{2A(0.332)^2}{Pr} \tag{33}$$

The extrapolation to $\delta = \lambda$ gives $Pr \simeq 0.471$ slightly larger than the estimation by Cioni *et al.* [21] ($Pr \simeq 0.2$) or Verzicco *et al.* [22] ($Pr \simeq 0.3$).

4. A direct access to the development length

4.1. *By direct observation*

As many others, Puthenveettil *et al.* [19] remarked that plumes generally detach from the plates as vertical sheets, thus appearing as lines in the plates observations. But they were the only ones, to our knowledge, to measure the length of these lines on a wide range of Ra and Pr. We agree with them that it is the thin "local natural convection boundary layers" around the plumes "whose thickness essentially decides the heat flux in turbulent convection". We thus shall assimilate the mean distance between the plumes with the development length h.

As Puthenveettil *et al.* [19] remark, this mean distance is related to the total line length L_p they measured and the area S on which the measure is made through:

$$h = \frac{S}{L_p} \tag{34}$$

We can thus check the relation 19, looking at $L_p H/S$ *versus* Nu. It is shown on figure 3. Except for the two smallest Nu values, the results nicely align as a power law. A linear regression on the data gives $\alpha \simeq 0.76$ [20].

4.2. *Through simultaneous Nu and Re measurements*

Equations 26, 28, can be written in a different way, if the thermal dissipation is dominated by the boundary layer, thus in the GL cases (I) and (II). Then $Nu = H/\delta$ (we omit the constant factor 2), and, for $Pr < 1$:

$$\frac{U\delta^2}{h\kappa} = \frac{UH}{\kappa}\frac{1}{Nu^2}\frac{H}{h} = 1 \quad ; \quad \frac{H}{h} = \frac{Nu^2}{RePr} \tag{35}$$

while, for $Pr > 1$, as $\gamma = U/\lambda$ and $\lambda/\delta = Pr^{1/3}$:

$$\frac{\gamma\delta^3}{h\kappa} = \frac{\delta UH}{\lambda\kappa}\frac{1}{Nu^2}\frac{H}{h} = 1 \quad ; \quad \frac{H}{h} = \frac{Nu^2}{RePr^{2/3}} \tag{36}$$

Equations 35, 36, give direct access to the behavior of h, independent of our assumption, equation 19. Figures 4 and 5 show how they apply to the results of respectively XZ Wu, Chavanne

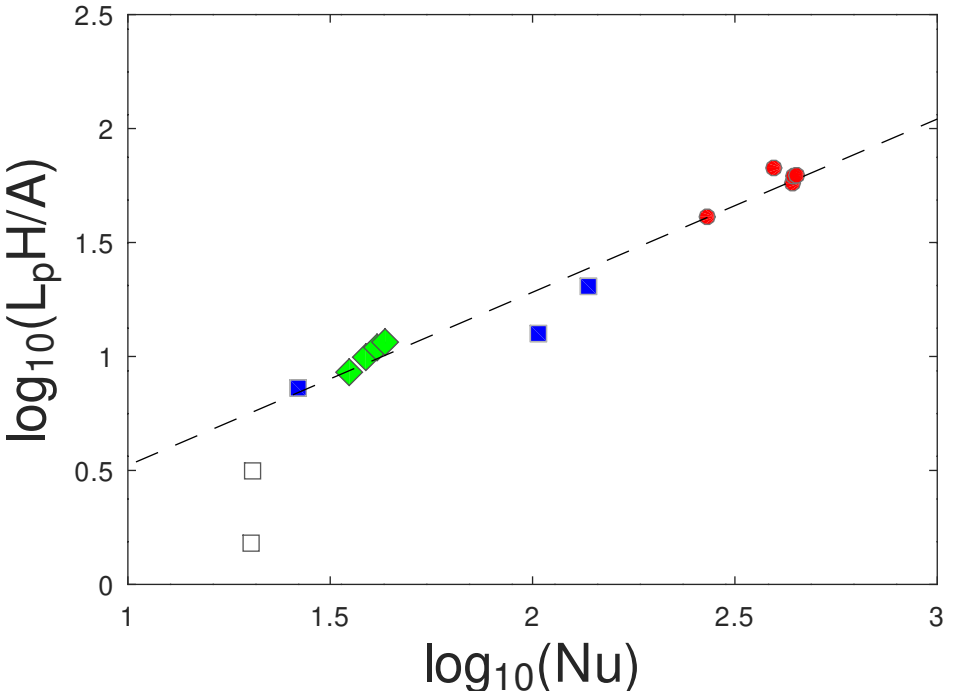

Figure 3. H/h, where h is the development length of the boundary layer for the Puthenveettil *et al.* results [19], versus the Nusselt number, in a logarithmic plot. It verifies equation 19 on a large range, with $\alpha \simeq 0.76$. diamonds: $Pr = 0.7$, squares: $Pr = 6$, circles: $Pr = 602$.

et al. and Musilova *et al.* . The former show a power law dependence of H/h versus Nu, on a large final range, in agreement with the postulated equation 19. A least squares regression for $\ln(Nu) > 3.3$ gives $\alpha \simeq 0.48$. The Chavanne *et al.* results show a transition between two such laws. A least squares regression for the lowest Nusselts gives $\alpha \simeq 0.30$. A least squares regression for $\ln(Nu) > 6$ gives $\alpha \simeq 0.77$, in agreement with the largest Nu values of the Musilova *et al.* results. The interest in Chavanne *et al.* set of data is the large span of Prandtl number values, which shows that no additional dependence with Pr exists out of the power law versus Nu.

As noted above, the temperature-velocity correlation coefficient χ can be considered as constant, at least within a given regime. In the expressions of H/h, it allows to replace $Nu/RePr$ by Θ/Δ. namely, for small Prandtl numbers:

$$\frac{H}{h} = Nu\frac{\Theta}{\Delta} \tag{37}$$

while, for large Prandtl numbers:

$$\frac{H}{h} = NuPr^{1/3}\frac{\Theta}{\Delta} \tag{38}$$

When the thermal dissipation is dominated by the boundary layer (cases I and II of GL), equations 37 and 38 have potentially another interpretation. Letting aside the Prandtl dependence, it can be written: $\delta\Delta = h\Theta$, as if the heat content of the thermal boundary layer would mix in a buffer layer of width h. This is close to the model proposed by Kadanoff *et al.* [10]. However, the Prandtl number dependence is hard to justify in this way.

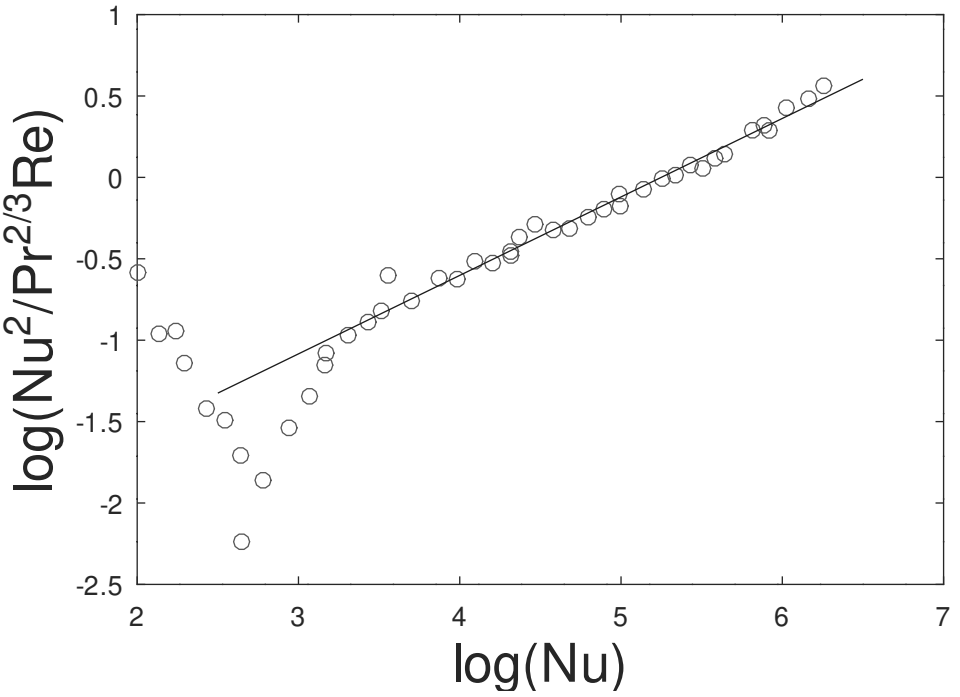

Figure 4. H/h, where h is the development length of the boundary layer for the XZ Wu results [11], versus the Nusselt number, in a logarithmic plot. It verifies equation 19 on a large range, with $\alpha \simeq 0.48$

4.3. *The α-spectrum*

We thus have an experimental confirmation of the conjecture made, equation 19, but no explanation. Indeed, the arguments presented by Kadanoff *et al.* [10] suggest that α should be equal to 0.5. The following discussion mainly reproduce these arguments, which have been extended to low Prandtl numbers by Cioni *et al.* [21].

The simplest interpretation of the development length h, is that it represents the mean distance between plumes. Let us assume with Kadanoff *et al.* that sheet-like plumes, of thickness λ develop. Within such a plume, the two last terms of the Navier-Stokes equation 1 should equilibrate. For small Prandtl numbers, this gives:

$$g\beta\Delta = \nu\frac{U}{\lambda^2} \tag{39}$$

This is equivalent to write that the buoyancy force $g\beta\Delta\lambda$, corresponding to the heat content $\Delta\lambda$, equilibrates with the viscous force $\nu U/\lambda$. Equation 39 gives:

$$\frac{g\beta\Delta H^3}{\nu\kappa} = Ra = \frac{\nu}{\kappa}\frac{UH}{\nu}\frac{H^2}{\lambda^2} = ReNu^2 \tag{40}$$

where we used the relation 29 between λ and δ for $Pr < 1$. Assuming that the bulk dominates the viscous dissipation:

$$RaNu = ReNu^3 = Re^3Pr^2 \tag{41}$$

Using equation 35:

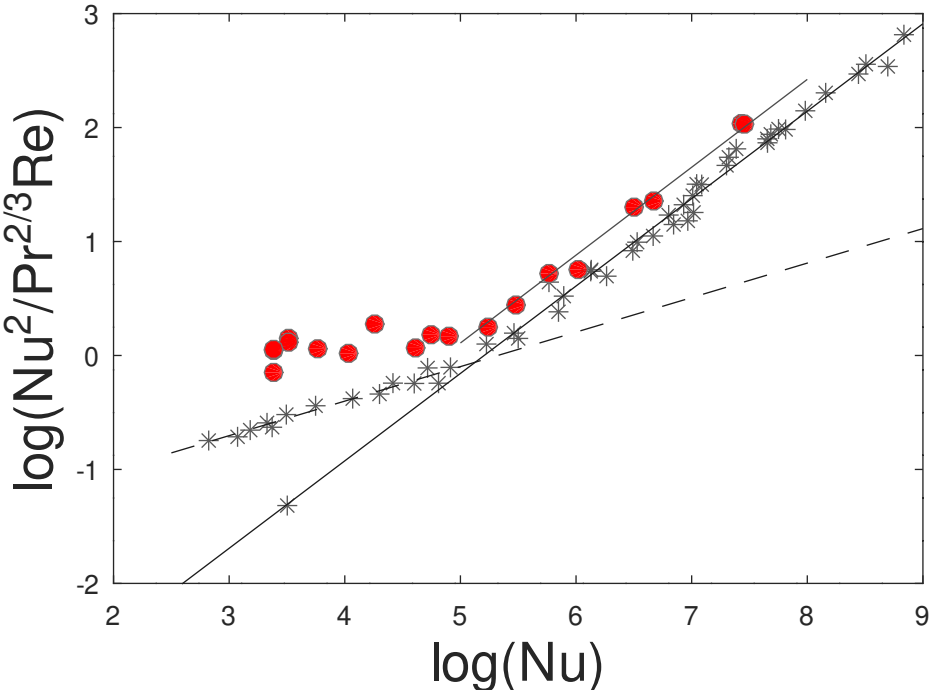

Figure 5. H/h, where h is the development length of the boundary layer for the Chavanne *et al.* results [14], asterisks, and the Musilova *et al.* ones [17], red circles, versus the Nusselt number, in a logarithmic plot. For Chavanne *et al.*, we have two regimes verifying equation 19, with respective slopes $\alpha \simeq 0.30$ and $\alpha \simeq 0.77$. The final regime of Musilova *et al.* is similar to the Chavanne *et al.* one

$$Nu^3 = Re^2 Pr^2 = Nu^{4-2\alpha} \tag{42}$$

and $\alpha = 0.5$

The argument differs somewhat for $Pr > 1$. Then, $\delta < \lambda$, and the heat content of the plume, of thickness λ, is only $\Delta\delta$. Equation 39 becomes:

$$g\beta\Delta\delta = \nu\frac{U}{\lambda} \tag{43}$$

Then:

$$\frac{g\beta\Delta H^3}{\nu\kappa} = Ra = \frac{\nu}{\kappa}\frac{UH}{\nu}\frac{H}{\lambda}\frac{H}{\delta} = Pr^{2/3}ReNu^2 \tag{44}$$

where we used the relation 30 between λ and δ for $Pr > 1$. Assuming again that the bulk dominates the viscous dissipation:

$$RaNu = Pr^{2/3}ReNu^3 = Re^3Pr^2 \tag{45}$$

Using equation 36:

$$Nu^3 = Re^2 Pr^{4/3} = Nu^{4-2\alpha} \tag{46}$$

and $\alpha = 0.5$. Moreover, in both cases, this model agrees with our assumption, equation 19.

The following argument could give an idea on the spectrum of other possible α values.

Let us call α_1 the first possible value for α. Above the transition from $\alpha = 0$ to $\alpha = \alpha_1$, as Nu increases, and δ goes down, the development length h could act as an effective large scale, the flow being confined between two neighboring plumes. Then, a new step of the instability of the thermal boundary layer could develop, yielding a new development length h'. The relation between h and h' would then write:

$$\frac{h}{h'} = \left(\frac{h}{\delta}\right)^{\alpha_1} \tag{47}$$

or:

$$\frac{h}{H}\frac{H}{h'} = Nu^{-\alpha_{n-1}}\frac{H}{h'} = \left(\frac{h}{H}\frac{H}{\delta}\right)^{\alpha_1} = \left(Nu^{1-\alpha_{n-1}}\right)^{\alpha_1} \tag{48}$$

It gives the following recursion formula:

$$(1-\alpha_n) = (1-\alpha_{n-1})(1-\alpha_1) \tag{49}$$

Identifying the Kadanoff α value, 0.5, with α_1, the following value would be 0.75, very close to the observed ones, 0.77 for the Chavanne *et al.* [14] or Musilova *et al.* [17] data, or 0.76 for the Puthenveettil *et al.* [19] ones .

Note that for the lowest α value observed, 0.30, the viscous dissipation is dominated by the boundary layer, in contradiction with the hypothesis of the Kadanoff *et al.* model [10], [21].

5. The viscous dissipation

In this section we shall determine the viscous dissipation in the velocity boundary layer, and in the bulk. Using then equation 12, we shall identify $(Nu-1)$ with Nu, as the difference is smaller than the error bar in the experimental or numerical studies of the concerned regimes. A constant reference for the mean viscous dissipation per unit mass will be:

$$\frac{U^3}{H} = \frac{\kappa^3}{H^4}Re^3Pr^3 \tag{50}$$

5.1. *The boundary layer contribution*

We have here to distinguish between a Blasius type boundary layer and a logarithmic one.

5.1.1. *The Blasius case*

Then, λ, the width of the velocity boundary layer, is the momentum diffusion length during a time h/U:

$$\lambda = \sqrt{\frac{\nu h}{U}} = HNu^{-\alpha/2}Re^{-1/2} \tag{51}$$

$$\gamma = \frac{U}{\lambda} = \frac{\nu}{H^2}Nu^{\alpha/2}Re^{3/2} \tag{52}$$

The boundary layer contribution to the viscous dissipation per unit mass will thus be:

$$\varepsilon_{bl} = \frac{\lambda}{H}\nu\gamma^2 = \frac{\nu^3}{H^4}Nu^{\alpha/2}Re^{5/2} \tag{53}$$

When this contribution dominates, comparing with equation 12 gives:

$$RaNu = Nu^{\alpha/2}Re^{5/2}Pr^2 \tag{54}$$

Another expression can be derived in this Blasius case. Namely:

$$\varepsilon_{bl} = \frac{\lambda}{H}\nu\frac{U^2}{\lambda^2} = \frac{\nu^3}{H^4}Re^2\frac{H}{\lambda} \tag{55}$$

Assuming that both the thermal and the viscous dissipations are dominated by the boundary layer, and using equations 12, 29 and 30, it gives, for small Prandtl numbers:

$$RaNu = NuRe^2Pr^{3/2} \tag{56}$$

and for large Prandtl numbers:

$$RaNu = NuRe^2Pr^{5/3}. \tag{57}$$

These expressions have the advantage to be independent of α.

5.1.2. *The logarithmic case*

Again, we have to take into account the development length h. In the viscous sublayer, the horizontal velocity component is $u_x = \gamma z$, with:

$$\gamma = v_*^2/\nu, \tag{58}$$

the transverse momentum flux being ρv_*^2 by definition of v_*. As above, the vertical velocity component u_z can be derived from the incompressibility relation 2:

$$\partial_z u_z = -\partial_x u_x = \frac{\gamma z}{h} \quad ; \quad u_z = \frac{\gamma z^2}{h} \tag{59}$$

(we omit the factor 2).

In the logarithmic range (see, for instance, [23]),

$$\partial_z u_x = \frac{v_*}{z} \quad ; \quad u_x = v_*\ln\left(\frac{v_* z}{\nu}\right) \quad ; \quad U = v_*\ln(Re) \tag{60}$$

(we omit the von Karman constant).

The velocity sublayer limit $z = \lambda$ corresponds to the transition viscous-convective for the momentum flux. In the convective region, $\langle u_x u_z\rangle = v_*^2 \simeq \sqrt{\langle u_x^2\rangle\langle u_z^2\rangle}$, assuming again a constant correlation coefficient. In the viscous region, $\sqrt{\langle u_x^2\rangle} \simeq \gamma z$, $\sqrt{\langle u_z^2\rangle} \simeq \gamma z^2/h$. Thus, at the transition:

$$v_*^2 = \frac{\gamma^2\lambda^3}{h} \quad ; \quad \frac{v_*^3\lambda^3}{\nu^3} = y_+^3(\lambda) = \frac{v_* h}{\nu} = \frac{ReNu^{-\alpha}}{\ln(Re)} = D \tag{61}$$

$y_+ = v_* z/\nu$ being the traditional notation for the reduced distance to the plate [23].

The above result strongly suggest that $D = 1$. Indeed, to our knowledge, no experimental results show a dependence of the reduced distance y_+ at the top of the viscous sublayer with the Reynolds number. This is the option we shall take.

Then the contribution of the viscous sublayer to the viscous dissipation is:

$$\frac{\lambda}{H}\nu\gamma^2 = \frac{v_*^3}{H} = \frac{U^3}{H(\ln Re)^3} \tag{62}$$

while that of the logarithmic part is:

$$\frac{1}{H}\int_\lambda^H \langle u_x u_z\rangle\,\partial_z u_x\,dz = \frac{v_*^3}{H}\ln Re = \frac{U^3}{H(\ln Re)^2} \tag{63}$$

The later being larger, we shall take it as the contribution of the logarithmic boundary layer. If it dominates the total viscous dissipation, we have:

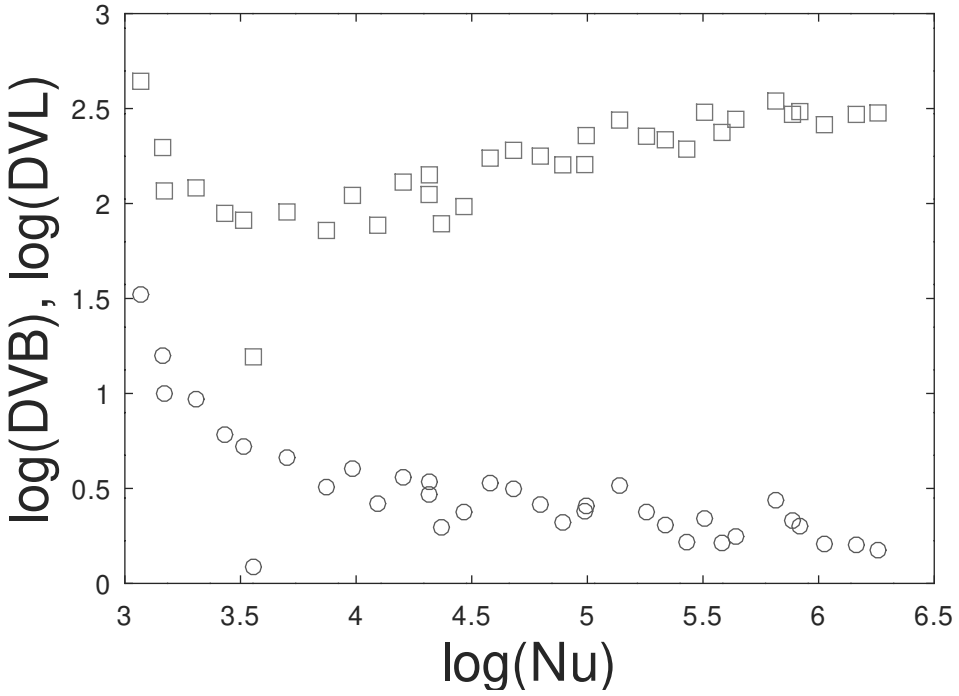

Figure 6. The respective parts of the viscous dissipation in the bulk (DVB, squares), and in the boundary layer (DVL, circles), for the X.Z. Wu results, using the value of α determined above. A vertical shift has been applied for clarity.

$$RaNu = \frac{Re^3 Pr^2}{(\ln Re)^2} \tag{64}$$

5.2. *The bulk contribution*

In the bulk, we shall follow the estimation by GL [7] and determine the bulk contribution as U^3/H, both in the Blasius and in the logarithmic cases. It comes from the interaction between rising and falling plumes. If this contribution dominates, we have:

$$RaNu = Re^3 Pr^2 \tag{65}$$

We can now compare with the experimental results. Indeed, the quantity:

$$DVB = \frac{Re^3 Pr^2}{RaNu} \tag{66}$$

represents, within a constant factor, the part of the viscous dissipation which is due to the bulk, while the quantity:

$$DVL = \frac{Nu^{\alpha/2} Re^{5/2} Pr^2}{RaNu} \tag{67}$$

represents, again within a constant factor, the part of the viscous dissipation which is due to the boundary layer. We let aside, for the moment, the logarithmic boundary layer case.

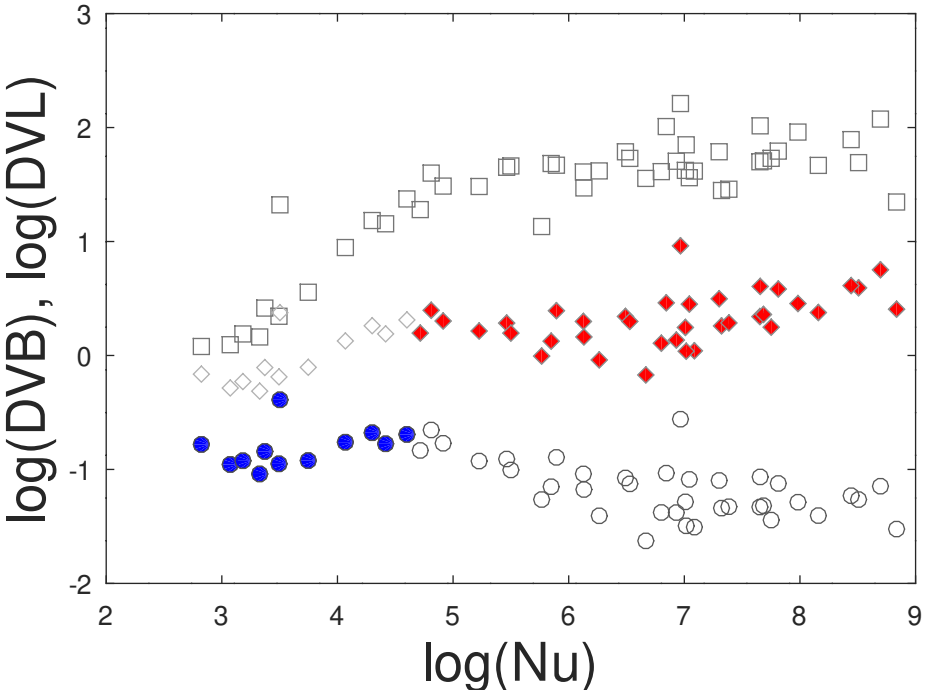

Figure 7. The respective parts of the viscous dissipation in the bulk (DVB, squares), and in the boundary layer (DVL, circles), for the Chavanne *et al.* results, using the two values of α determined above. The full symbols underline the two respective ranges. A vertical shift has been applied for clarity.

On figure 6, we show these two quantities, versus the Nusselt number, in logarithmic scales, for the X.Z. Wu results. None of these quantity shows a plateau. The part of the bulk dissipation increases with Nu, while the part of the boundary layer decreases. This is an excellent illustration of the GL point of view, a slow cross-over between the two regimes.

On figure 7, we show the same quantities, versus the Nusselt number, in logarithmic scales, for the Chavanne *et al.* results. While it is clear that the first regime, with $\alpha = 0.30$, is dominated by the boundary layer, the second regime seems to give a plateau in both cases. We are unable to decide between the bulk or the boundary layer dominating the viscous dissipation. This will be possible only later, considering the consequences for the temperature fluctuations.

6. The thermal boundary layer δ

Indeed, the determination of λ in the previous section gives the thermal boundary layer δ as a by-product. Let us first recall the results for λ. In the Blasius case:

$$\lambda = HNu^{-\alpha/2}Re^{-1/2} \tag{68}$$

while, in the logarithmic boundary layer case:

$$\lambda = \frac{\nu}{v_*} = H\frac{\ln(Re)}{Re} \tag{69}$$

Following our previous analysis, for small Prandtl numbers:

$$\delta = \frac{\lambda}{Pr^{1/2}} \tag{70}$$

while, for large Prandtl numbers:

$$\delta = \frac{\lambda}{Pr^{1/3}} \tag{71}$$

Some caution, however, must be taken in the logarithmic case (and if $\alpha \simeq 1$). As remarked above, our analysis is valid only if $h >> \delta$. In the logarithmic case, the velocity vertical component fluctuation does not grow when $z > \lambda$, and remains of order v_*. For low Prandtl numbers in the logarithmic case, it implies:

$$\delta = \frac{\lambda}{Pr} \tag{72}$$

For large Prandtl numbers in the same case, let us remark that equation 23 implies, when $h \simeq \delta$:

$$\delta^2 = \frac{\kappa}{\gamma} \tag{73}$$

Then, using equation 58:

$$\delta^2 = \frac{\kappa\nu}{v_*^2} = \frac{\lambda^2}{Pr} \tag{74}$$

Note that Kraichnan [24] obtained the same relation, assuming that the vertical velocity fluctuation is linear in z for $z < \lambda$, at least for not too small z.

7. The thermal dissipation

7.1. *The boundary layer contribution*

When the thermal dissipation is dominated by the boundary layer, equation 13 yield to an identity. We could refer to our determination of the boundary layer δ, for instance through equation 35 or 36, but we must remember that we used it to determine α, and thus it is identically verified.

The only check we have is thus to look at the bulk contribution. If the bulk contribution is constant, we shall conclude that it dominates the thermal dissipation. If it is not constant, we shall conclude that a significant boundary layer contribution exists. We have no possible cross-check.

7.1.1. *The temperature profile*

Moreover, considering that the boundary layer contribution is only part of the total thermal dissipation implies that the temperature difference across the boundary layer, $\Delta^*/2$, differs from $\Delta/2$. Let us call Nu^* the boundary layer contribution to the thermal dissipation B_{th} normalised by $\kappa(\Delta/H)^2$:

$$B_{th} = \frac{\kappa}{4}\left(\frac{\Delta^*}{H}\right)^2 \frac{2\delta}{H} = \frac{\kappa\Delta^2}{H^2}\left(\frac{\Delta^*}{\Delta}\right)^2 \frac{H}{2\delta} \tag{75}$$

As:

$$\frac{\Delta^*}{\Delta} = \frac{2\delta}{H} Nu \tag{76}$$

we have:

$$Nu^* = \frac{\Delta^*}{\Delta} Nu \tag{77}$$

which means that the boundary layer contribution is in the same proportion as the temperature differences. It is then interesting to look at the temperature profile in the convective part of the convection cell.

The situation is indeed very similar to that yielding to the turbulent logarithmic velocity profile. $\Theta = \Delta Nu/RePr$ acts as a typical temperature difference, while, at a distance z from the plate, there is no other characteristic length than z. From dimensional analysis, the mean vertical temperature gradient must write:

$$\langle \frac{\partial T}{\partial z} \rangle = \varpi \frac{\Theta}{z} \tag{78}$$

where ϖ is a universal constant, similar to the von Karman constant. Then $\langle T \rangle = \varpi \Theta \ln(z) + cst$ and $\Delta - \Delta^* \simeq \varpi \Theta \ln(Nu)$. Note that such a logarithmic temperature profile has been effectively observed in some studies [25].

Thus, the evolution is slow, and Δ cannot be much larger than Δ^* before extremely large values of Nu be reached. In practical situations, the boundary layer contribution is always a noticeable part of the total thermal dissipation. Rather than a dissipation "dominated" by the bulk, we should speak of a dissipation "driven" by the bulk, as the boundary layer adapts to follow the bulk contribution.

7.2. *The bulk contribution*

Following the approach of [9], we shall determine the bulk contribution to the thermal dissipation through:

$$\kappa \langle \partial_i T \partial_i T \rangle \simeq \kappa \left(\frac{\vartheta}{\sigma} \right)^2 \tag{79}$$

where ϑ is the temperature fluctuation at the thermal dissipative scale σ. As in [9], we have to distinguish between hard and soft turbulence, and large or small Prandtl numbers.

7.2.1. *Small Prandtl numbers. Hard turbulence.*

When the inertial turbulent cascade is sufficiently developed, the thermal dissipative scale σ, while larger than the viscous one η ($Pr < 1$), is in the inertial range: $H > \sigma > \eta$. At the scale σ, the thermal diffusion time is equal to the stretching time. Put in other words, the Peclet number is 1:

$$\frac{\kappa}{\sigma^2} = \frac{v_\sigma}{\sigma} \tag{80}$$

Using the Kolmogorov 41 theory [26]:

$$\frac{H}{\sigma} = \frac{H}{\kappa} U \left(\frac{\sigma}{H} \right)^{1/3} \quad ; \quad \frac{H}{\sigma} = \left(\frac{UH}{\kappa} \right)^{3/4} = (RePr)^{3/4} \tag{81}$$

As for the temperature fluctuations:

$$\vartheta = \Theta \left(\frac{\sigma}{H} \right)^{1/3} = \Theta (RePr)^{-1/4} \tag{82}$$

Using equations 79 and 15, the bulk contribution to the thermal dissipation is then:

$$\kappa\left(\frac{\Delta}{H}\right)^2\left(\frac{\Theta}{\Delta}\right)^2 (RePr)^{-1/2}(RePr)^{3/2} =$$
$$= \kappa\left(\frac{\Delta}{H}\right)^2 \frac{Nu^2}{RePr} \tag{83}$$

Note that we could have obtained this result, identifying the thermal dissipation ϵ_T with $U\Theta^2/H$, as GL did [7]. $U\Theta^2/H$ is the large scale expression of ϵ_T, and the cascade ensures the conservation of ϵ_T:

$$\frac{U\Theta^2}{H} = \kappa\left(\frac{\Delta}{H}\right)^2 \frac{UH}{\nu}\frac{\nu}{\kappa}\frac{\Theta^2}{\Delta^2} \tag{84}$$

If this contribution dominates, using equation 13 gives:

$$Nu = RePr \quad ; \quad \frac{\Theta}{\Delta} = cst \tag{85}$$

7.2.2. *Small Prandtl numbers. Intermediate turbulence.*

For smaller Reynolds numbers, the thermal dissipative scale σ is out of the inertial range. Then, we must identify it with H. The bulk contribution to the thermal dissipation is then:

$$\kappa\left(\frac{\Theta}{H}\right)^2 = \kappa\left(\frac{\Delta}{H}\right)^2\left(\frac{\Theta}{\Delta}\right)^2 = \kappa\left(\frac{\Delta}{H}\right)^2\left(\frac{Nu}{RePr}\right)^2 \tag{86}$$

If this contribution dominates, using equations 13 gives:

$$Nu = (RePr)^2 = (RaPr)^2 \quad ; \quad \frac{\Theta}{\Delta} = RePr \tag{87}$$

7.2.3. *Large Prandtl numbers. Hard turbulence.*

In this case, an inertial range exists, but the thermal dissipative scale σ is smaller than the viscous dissipation scale η. These scales are related through:

$$\frac{\kappa}{\sigma^2} = \frac{v_\sigma}{\sigma} = \frac{v_\eta}{\eta} = \frac{\nu}{\eta^2} \tag{88}$$

This regime is known as the Batchelor regime [9]. The temperature fluctuation at the thermal dissipative scale σ is the same as at the viscous dissipative scale η:

$$\vartheta = \Theta\left(\frac{\eta}{H}\right)^{1/3} = \Theta Re^{-1/4} \tag{89}$$

The bulk contribution to the thermal dissipation is then:

$$\kappa\left(\frac{\vartheta}{\sigma}\right)^2 = \kappa\left(\frac{\Delta}{H}\right)^2\left(\frac{\Theta}{\Delta}\right)^2\left(\frac{\vartheta}{\Theta}\right)^2\left(\frac{H}{\eta}\right)^2\left(\frac{\eta}{\sigma}\right)^2$$
$$= \kappa\left(\frac{\Delta}{H}\right)^2\left(\frac{\Theta}{\Delta}\right)^2 RePr \tag{90}$$

This result is identical to what we obtained in the low Prandtl numbers case, equation 84, for the same reasons. It then raises a problem when both dissipations, thermal and viscous, are dominated by the bulk (GL case IV). The two equations 85 and 65 then give:

$$Re = Ra^{1/2}Pr^{-1/2} \quad ; \quad Nu = Ra^{1/2}Pr^{1/2} \tag{91}$$

This cannot be true, as it violates, for sufficiently large Prandtl number, the result of Doering and Constantin [6]. These authors have derived an absolute majoration of the Nusselt number:

$$Nu < CRa^{1/2} \tag{92}$$

where C is a constant.

We think that the solution of this paradox is as follows:

At large Prandtl numbers, the heat diffusivity is smaller than the velocity one. When a plume raises, generally having a sheet shape, it drags the fluid on a width larger than the plume one. The width of the velocity profile is $Pr^{1/2}$ times larger than the temperature one. Let us call θ_m the average temperature on the width of the temperature profile. The average temperature in the whole dragged fluid will be $< \theta >= \theta_m / Pr^{1/2}$. In the same way, the average temperature squared in the whole dragged fluid will be $< \theta^2 >= \theta_m^2 / Pr^{1/2} =< \theta >^2 Pr^{1/2}$. As the relation $\Theta = \Delta Nu/(RePr)$ seems firmly established, we must consider that, at large Prandtl numbers:

$$\frac{\langle\theta^2\rangle}{\Delta^2} = \frac{Nu^2}{Re^2 Pr^{3/2}} \tag{93}$$

and the bulk thermal dissipation is:

$$\kappa \left(\frac{\Delta}{H}\right)^2 \frac{Nu^2}{Re^2 Pr^{3/2}} RePr = \kappa \left(\frac{\Delta}{H}\right)^2 \frac{Nu^2}{RePr^{1/2}} \tag{94}$$

Note that Lohse and Shishkina [5] solve the same paradox in an apparently different way. If this contribution dominates, we have:

$$Nu = RePr^{1/2} \quad ; \quad \frac{\Theta}{\Delta} = Pr^{-1/2} \tag{95}$$

and the two equations 95 and 65 give:

$$Re = Ra^{1/2} Pr^{-3/4} \quad ; \quad Nu = Ra^{1/2} Pr^{-1/4} \tag{96}$$

now in agreement with the Doering and Constantin majoration [6].

7.2.4. *Arbitrary Prandtl numbers. Soft turbulence.*

In this case, while turbulent, the bulk has no inertial energy cascade. As in [9], we then determine the temperature dissipation scale σ, writing that the inverse temperature diffusion time is equal to the velocity gradient, itself determined through the dissipation:

$$\frac{\kappa}{\sigma^2} = \sqrt{\frac{\varepsilon}{\nu}} \tag{97}$$

The bulk contribution to the thermal dissipation is then, for large Prandtl numbers:

$$\begin{aligned} \kappa \frac{\langle\theta^2\rangle}{\sigma^2} &= \langle\theta^2\rangle \sqrt{\frac{\varepsilon}{\nu}} \\ &= \Delta^2 \frac{Nu^2}{Re^2 Pr^{3/2}} \sqrt{\frac{\kappa^3 Re^3 Pr^3}{H^4 \nu}} \\ &= \kappa \left(\frac{\Delta}{H}\right)^2 \frac{Nu^2}{Re^{1/2} Pr^{1/2}} \end{aligned} \tag{98}$$

and for small Prandtl numbers:

$$\kappa \frac{\langle\theta^2\rangle}{\sigma^2} = \kappa \left(\frac{\Delta}{H}\right)^2 \frac{Nu^2}{Re^{1/2} Pr} \tag{99}$$

If this contribution dominates, we have:

$$Nu = Re^{1/2} Pr^{1/2} \quad ; \quad \frac{\Theta}{\Delta} = Nu^{-1} \tag{100}$$

for large Prandtl numbers, and:

$$Nu = Re^{1/2} Pr \quad ; \quad \frac{\Theta}{\Delta} = Pr Nu^{-1} \tag{101}$$

for small Prandtl numbers. If the bulk viscous dissipation also dominates (GL case IV_u), the equations 100 , 101 and 65 give:

$$Re = Ra^{2/5} Pr^{-3/5} \quad ; \quad Nu = Ra^{1/5} Pr^{1/5} \tag{102}$$

for large Prandtl numbers, and:

$$Re = Ra^{2/5} Pr^{-2/5} \quad ; \quad Nu = Ra^{1/5} Pr^{4/5} \tag{103}$$

for small Prandtl numbers.

8. Discussion

We can now obtain the scalings of Nu, Re, and Θ/Δ in all "pure" regimes. Such an enumeration would however be tedious, as we have to distinguish not only all the GL regimes, but also if the Prandtl number is large or small, if the boundary layer is Blasius or logarithmic, and if the turbulence in the bulk is hard or soft. We prefer to detail some remarkable cases, to show how these scalings can be obtained.

8.0.1. *The Kadanoff solution.*

This case corresponds to a bulk dominated viscous dissipation, and a thermal dissipation dominated by a Blasius boundary layer. The value of α is $\alpha = 1/2$.

Equation 65 gives:

$$RaNu = Re^3 Pr^2 \tag{104}$$

At large Prandtl number, equations 68 and 71 give:

$$\begin{aligned} Nu &= \frac{H}{\delta} = Nu^{\alpha/2} Re^{1/2} Pr^{1/3} \\ Nu &= Re^{1/(2-\alpha)} Pr^{2/3(2-\alpha)} \end{aligned} \tag{105}$$

Then:

$$Re = Ra^{(2-\alpha)/(5-3\alpha)} Pr^{-2/3} \tag{106}$$

$$Nu = Ra^{1/(5-3\alpha)} \tag{107}$$

$$\frac{\Theta}{\Delta} = Ra^{(\alpha-1)/(5-3\alpha)} Pr^{-1/3} \tag{108}$$

which, for $\alpha = 1/2$, gives:

$$Re = Ra^{3/7} Pr^{-2/3} \; ; \; Nu = Ra^{2/7} \; ; \; \frac{\Theta}{\Delta} = Ra^{-1/7} Pr^{-1/3} \tag{109}$$

The Cioni *et al.* [21] extension of this regime to small Prandtl numbers corresponds to using equation 70 instead of 71:

$$Nu = \frac{H}{\delta} = Nu^{\alpha/2} Re^{1/2} Pr^{1/2}$$
$$Nu = Re^{1/(2-\alpha)} Pr^{1/(2-\alpha)} \tag{110}$$

Then:

$$Re = Ra^{(2-\alpha)/(5-3\alpha)} Pr^{-(3-2\alpha)/(5-3\alpha)} \tag{111}$$
$$Nu = Ra^{1/(5-3\alpha)} Pr^{1/(5-3\alpha)} \tag{112}$$
$$\frac{\Theta}{\Delta} = Ra^{(\alpha-1)/(5-3\alpha)} Pr^{(5\alpha-1)/(5-3\alpha)} \tag{113}$$

which, for $\alpha = 1/2$, gives:

$$Re = Ra^{3/7} Pr^{-4/7} \; ; \; Nu = Ra^{2/7} Pr^{2/7} \; ; \; \frac{\Theta}{\Delta} = Ra^{-1/7} Pr^{3/7} \tag{114}$$

8.0.2. *The Kraichnan solution.*

In a celebrated paper [24], R. Kraichnan proposed a large Rayleigh numbers regime for moderately large Prandtl numbers, which has long been understood as the "ultimate" regime. However, as each thermal boundary layer is supposed to have half the total temperature difference Δ across it, this regime corresponds to II_u in the GL classification, with logarithmic velocity boundary layers.

On the one hand, we again have, using equation 65:

$$RaNu = Re^3 Pr^2 \tag{115}$$

On the other hand, using equations 74 and 69 we obtain:

$$Nu = \frac{H}{\delta} = \frac{RePr^{1/2}}{\ln(Re)} \tag{116}$$

It gives:

$$Re = \frac{Ra^{1/2} Pr^{-3/4}}{(\ln(Re))^{1/2}} \tag{117}$$
$$Nu = \frac{Ra^{1/2} Pr^{-1/4}}{(\ln(Re))^{3/2}} \tag{118}$$
$$\frac{\Theta}{\Delta} = \frac{Pr^{-1/2}}{\ln(Re)} \tag{119}$$

which is the result of Kraichnan.

8.0.3. *The observation of Cioni et al..*

During one of the runs of their mercury experiment, Cioni *et al.* [21] observed a rapid increase of the Nusselt number on a limited range of Rayleigh numbers. Their interpretation was a transition between two regimes. However, as shown on the figure 8, this rapid increase nicely fits with the predicted behavior, equation 87, in a GL case IV_l, and intermediate turbulence.

This regime would be much better characterized if Cioni *et al.* could have measured the Reynolds number or/and the temperature fluctuations simultaneously with these observations. A behavior $Nu \propto Ra^2$ is however sufficiently unusual. Moreover, just before this rapid increase, Cioni *et al.* observed a regime $Nu \propto Ra^{1/5}$, which agrees with the low Prandtl number soft turbulence, equation 103. The transition between this regime and the rapid increase of Nu would

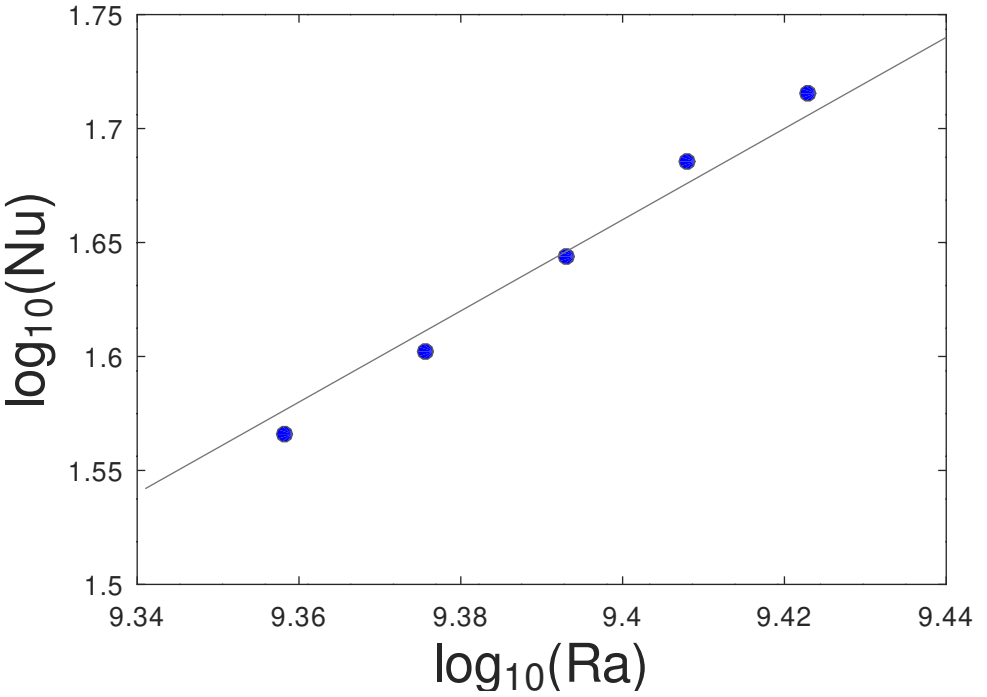

Figure 8. Part of the Cioni *et al.* results [21], corresponding to their "rapid increase" in Nusselt number, in logarithmic coordinates. The continuous line has a slope 2.

thus correspond to the transition soft to hard turbulence *i.e.* the apparition of an inertial cascade. It strongly suggest that the Cioni *et al.* observation is the only known observed regime of type IV in the GL classification.

8.0.4. *The observation of Chavanne et al.*.

Except the Cioni *et al.* observation discussed above, Chavanne *et al.* [14] were the first to observe a logarithmic slope μ of Nu *versus* Ra larger than 1/3. As a tentative interpretation, they assimilated this regime with the Kraichnan regime. However, the observed μ was smaller than 1/2, which could be attributed to the logarithmic corrections. Later, other authors [27] observed a transition toward a regime with a similar value for μ, larger than 1/3 but smaller than 1/2, while at much higher Rayleigh number.

Indeed, a logarithmic correction is hardly distinguishable from a power law with a small exponent, and even the power law observed on figure 5 for the second regime could dissimulate a logarithmic correction. Let us however look at equations 105 and 116. They both give Nu as the product of a function of Re and a power of Pr. As $\ln(Re)$ mimics a power law, the behavior of the different functions of Re should be close. For the final regime of Chavanne *et al.*, the exponent of Re, $1/(2-\alpha) \simeq 0.81$, and $Nu/Re^{0.81}$ should be poorly dependent on Re at constant Pr.

We then select the data for which $3 \cdot 10^5 < Re < 6 \cdot 10^5$, and plot:

$$\frac{Nu}{Re^{0.81} Pr^{1/2}} \tag{120}$$

versus the Prandtl number, in logarithmic coordinates (see figure 9). It would give a constant value if the original result of Kraichnan is the good candidate. It would give an ascending slope:

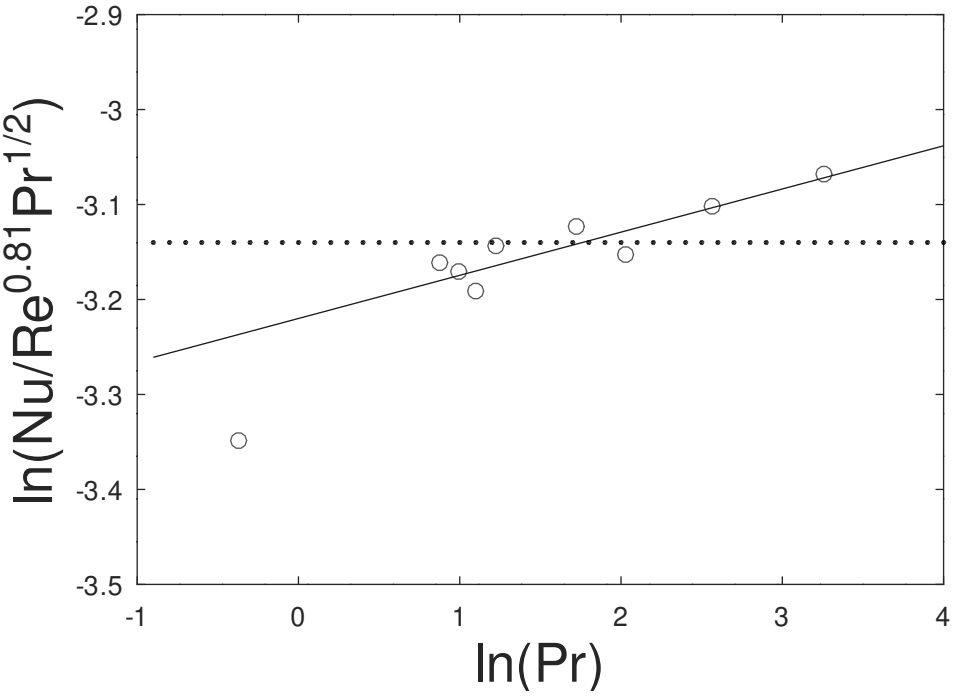

Figure 9. Dependence of the Nusselt number at "constant" Reynolds number($3\cdot10^5 < Re < 6\cdot10^5$), for the Chavanne *et al.* results [14]. The constant dotted line corresponds to the Kraichnan [24] solution. The continuous line corresponds to the Blasius boundary layer, with $\alpha = 0.77$ (see text).

$$\frac{2}{3(2-\alpha)} - \frac{1}{2} \simeq 0.042 \tag{121}$$

in the Blasius case. The results seem to favor the last case.

Does the more recent results [27] correspond to the Blasius or the logarithmic case? It can only be decided through a similar test, involving a large range of Prandtl numbers.

9. Conclusion

According to the present work, the various Rayleigh-Bénard convection regimes can be separated in two kinds:

- The unscaling ones. Either because of a transition between two scaling regimes, or due to a special organization of the flow to be elucidated, the cross-correlation coefficient between velocity and temperature cannot be considered as constant. A fundamental hypothesis of most of the proposed models then fails. One can then only rely to the GL theory [7] . Even if their estimation of the boundary layer viscous dissipation appears as too crude, the more elaborated evaluations, like equation 53, are always intermediate between the crude estimation and the bulk dissipation. Thus, estimating the total dissipation as a pondered mean of these two extremes should correctly capture the physics.
- The scaling ones. Then, the cross-correlation coefficient between velocity and temperature can be considered as constant, and a deeper analysis can be performed. It reveals

that different regimes are possible, even for the same Rayleigh number Ra, Prandtl number Pr, and aspect ratio Γ. It also reveals that the evolution of the viscous boundary layer proceeds through a succession of steps toward the turbulent state, rather than through an abrupt and single transition.

One could wonder why we mainly used relatively old experimental results, while more recent, often more precise works exist [27], [28], [29], including numerical ones [30], [31]. The reason is that these works do not provide simultaneous measurements of Nu, Re and Θ. Different regimes have been observed, at the same Rayleigh and Prandtl numbers, even in the same cell. So, simultaneous measurements are essentials. Except in very special cases, as the rapid increase observed by Cioni *et al.* [21], the behavior of the Nusselt number alone cannot allow to conclude.

The numerical works have the advantage to give access to all the possible measurements. However, for obvious reasons, they hardly give dense series in the Ra, Pr plane. As different regimes rapidly succeed each other, isolated measurements again cannot allow to conclude.

Let us enumerate some aspects of Rayleigh-Bénard convection on which our study gives a new point of view:

- Several studies on two dimensional (2D) Rayleigh-Bénard convection have pointed the remarkable similitude with three dimensions (3D). Indeed, up to the Soft Turbulence included, there are no real difference between 2D and 3D. Only in the Hard Turbulence regime, the energy or enstrophy cascades are dramatically different in 2D and in 3D. In particular, equations 12 and 13 are valid in 2D. The fact that similar high Rayleigh number regimes have been observed both in 2D numerical studies [32] and in 3D experimental ones [14], [27], strongly suggests that all these regimes rely to the category II in the GL classification, and not to an "ultimate" regime.
- In our point of view, most of the transitions in the cell behavior result from an abrupt change in the structure of the boundary layer. This is exactly the conclusion of Gauthier *et. al.* [33] about the Chavanne observation. They observe that, after the transition, the spectrum of plate temperature fluctuations extends to much higher frequencies, which is coherent with a much smaller development length h.
- Temperature fluctuations measurements are generally easier and more reliable than velocity measurements. Assuming the constancy of the cross-correlation coefficient between vertical velocity and temperature (an assumption implicitely made in all models) gives indirectly access to the Reynolds number through temperature measurements. We urge all experimentalists to include these temperature fluctuations in their data.

10. Acknowledgments

The authors are thankful to Marc Moulin and his team at the mechanical workshop for the design and machining of the experimental apparatus, and funding from the ANR-22-CE30-0018-01 PRC “Thermal” project. This project was provided with computing HPC and storage resources by GENCI at CINES and TGCC thanks to the grants 2022, 2023 and 2024-2A00326 on the supercomputer Joliot Curie’s ROME and Adastra’s GENOA partitions. We thank Vera Musilová, Michal Macek and Pavel Urban for sharing their data table with us.

References

[1] G.I. Barenblatt, "Scaling, self-similarity, and intermediate asymptotics", Cambridge University Press, (1996).
[2] D. Lohse, K.-Q. Xia, "Small-scale properties of turbulent Rayleigh-Bénard convection", Annu. Rev. Fluid Mech. **42** 335–64, (2010)
[3] F. Chillà, J. Schumacher, "New perspectives in turbulent Rayleigh-Bénard convection", Eur. Phys. J. **E 35**, 1-25, (2012).

[4] G. Ahlers, S. Grossmann, D. Lohse, "Heat transfer and large scale dynamics in turbulent Rayleigh-Bénard convection", Reviews of modern physics **81**, 503, (2009).

[5] D. Lohse, O. Shishkina, "Ultimate Rayleigh-Bénard turbulence", Reviews of modern physics **96**, 035001, (2024).

[6] C. R. Doering and P. Constantin, "Variational bounds on energy dissipation in incompressible flows. III. Convection", Phys. Rev. E **53**, 5957 (1996).

[7] S. Grossmann, D. Lohse, "Scaling in thermal convection: a unifying theory", J. Fluid Mech. **407**, 27-56, (2000). For the last version, see: R.J.A.M. Stevens, E.P. van der Poel, S. Grossmann and D. Lohse, "The unifying theory of scaling in thermal convection: the updated prefactors" J. Fluid Mech. **730**, 295, (2013).

[8] Paul E. Dimotakis "The mixing transition in turbulent flows" J. Fluid Mech., **409**, 69, (2000).

[9] B. Castaing, E. Rusaouën, J. Salort, and F. Chillà, "Turbulent heat transport regimes in a channel", Phys. Rev. Fluids **2**, 062801 (2017)

[10] B. Castaing, G. Gunaratne, F. Heslot, L. Kadanoff, A. Libchaber, S. Thomae, X. Z. Wu, S. Zaleski, and G. Zanetti, "Scaling of hard thermal turbulence in Rayleigh-Bénard convection",' J. Fluid Mech. **204**, 1 (1989).

[11] X. Z. Wu, "Along a road to developed turbulence: Free thermal convection in low temperature helium gas," Ph.D. thesis, University of Chicago, (1991).

[12] M. Belkadi, L. Guislain, A. Sergent, B. Podvin, F. Chillà, and J. Salort, "Experimental and numerical shadowgraph in turbulent rayleigh-bénard convection with a rough boundary: investigation of plumes", J. Fluid Mech. 895:A7 (2020)

[13] M. Belkadi, A. Sergent, Y. Fraigneau, and B. Podvin, "On the role of roughness valleys in turbulent Rayleigh-Bénard convection", J. Fluid Mech. 923:A6 (2021)

[14] X. Chavanne *et al.*, "Turbulent Rayleigh-Bénard convection in gaseous and liquid He", Phys.of Fluids **13** 1300 (2001).

[15] P.-E. Roche, B. Castaing, B. Chabaud, B. Hébral, and J. Sommeria, "Side Wall effects in Rayleigh-Bénard Experiments", E.P.J.**B 24** 405 (2001).

[16] G. Ahlers, "Effect of sidewall conductance on heat-transport measurements for turbulent Rayleigh-Bénard convection ", Phys. Rev. **E 63** 15303 (2001).

[17] V. Musilová, T. Králík, M. La Mantia, M. Macek, P. Urban and L. Skrbek "Reynolds number scaling in cryogenic turbulent Rayleigh–Bénard convection in a cylindrical aspect ratio one cell", J. Fluid Mech. , **832**, 721 (2017).

[18] Emily S. C. Ching, "Heat flux and shear rate in turbulent convection", Phys. Rev. E **55**, 1189 (1997)

[19] B. A. Puthenveettil, G. S. Gunasegarane, Y. K. Agrawal, D. Schmeling, J. Bosbach and J. H. Arakeri, "Length of near-wall plumes in turbulent convection", J. Fluid Mech., **685**, 335 (2011).

[20] In their paper [19], Puthenveettil *et al.* postulate that the Rayleigh number based on the distance between plumes, $Ra(h/H)^3$, only depends on Pr. They write it $Ra^{1/3}h/H \propto Pr^n$. Using equations 19, 36, and 54, it gives $\alpha = 0.8$ (very close to the 0.76 found above) and $n = 1/9$, close to the 0.1 they find.

[21] S. Cioni, S. Ciliberto and J. Sommeria, "Strongly turbulent Rayleigh-Bénard convection in mercury: comparison with results at moderate Prandtl number", J. Fluid Mech. , **335**, 111, (1997)

[22] R. Verzicco, R. Camussi, "Prandtl number effects in convective turbulence", J. Fluid Mech. , **383**, 55, (1999)

[23] E. Guyon, JP Hulin, L. Petit, "Hydrodynamique Physique" CNRS Editor, EDP Science, 3rd edition (2012)

[24] R. Kraichnan, "Turbulent Thermal Convection at Arbitrary Prandtl Number", Phys. of Fluids **5**, 1374, (1962).

[25] G. Ahlers, E. Bodenschatz, D. Funfschilling, S. Grossmann, X. He, D. Lohse, R.J.A.M. Stevens, and R. Verzicco, "Logarithmic temperature profiles of turbulent Rayleigh-Bénard convection in the classical and ultimate state for a Prandtl number of 0.8", J. Fluid Mech. **758** , 436 - 467, (2014).

[26] U. Frisch "Turbulence" Cambridge University Press, (1995).

[27] X. He, D. P. M. van Gils, E. Bodenschatz and G. Ahlers, "Reynolds numbers and the elliptic approximation near the ultimate state of turbulent Rayleigh–Bénard convection", New J. Phys. **17**, 063028, (2015).

[28] JJ Niemela, L Skrbek, KR Sreenivasan, RJ Donnelly, "Turbulent convection at very high Rayleigh numbers", Nature **404**, 837-840, (2000).

[29] P.-E. Roche, F. Gauthier, R Kaiser and J Salort, "On the triggering of the Ultimate Regime of convection", New Journal of Physics **12**, 085014, (2010).

[30] RJAM Stevens, D Lohse, R Verzicco, "Prandtl and Rayleigh number dependence of heat transport in high Rayleigh number thermal convection", J. Fluid Mech. **688**, 31-43, (2011).

[31] J Bailon-Cuba, MS Emran, J Schumacher, "Aspect ratio dependence of heat transfer and large-scale flow in turbulent convection", J. Fluid Mech. **655**, 152-173, (2010).

[32] X Zhu, V Mathai, RJAM Stevens, R Verzicco, D Lohse, "Transition to the ultimate regime in two-dimensional Rayleigh-Bénard convection", Phys. Rev. Lett. **120**, 144502 (2018).

[33] F. Gauthier and P.-E. Roche, "Evidence of a boundary layer instability at very high Rayleigh number", Europhys. Lett. **83**, 24005, (2008).

[34] L. Landau and E. Lifchitz, "Mécanique des Fluides", Editions Mir, Moscou (1971).